C2/c pyroxene from two alkaline sodic suites (Western Ross Embayment — Antarctica): crystal chemical characterization and its petrologic significance

GABRIELLA SALVIULO

Dipartimento di Mineralogia e Petrologia, Università di Padova, Corso Garibaldi 37, 35122 Padova, Italy

LUCIANO SECCO

Dipartimento di Mineralogia e Petrologia, Università di Padova, Corso Garibaldi 37, 35122 Padova, Italy

PAOLO ANTONINI

Dipartimento di Scienze della Terra, Università di Trieste, Via Weiss 8, 34127 Trieste, Italy

AND

ENZO MICHELE PICCIRILLO

Dipartimento di Scienze della Terra, Università di Trieste, Via Weiss 8, 34127 Trieste, Italy

Abstract

Two *C2/c* pyroxene suites from sodic alkaline rocks (Basanite-Phonolite: B-Ph and Alkali basalt-Trachyphonolite: AB-T) belonging to the McMurdo Volcanic Group (Mt. Melbourne province and Mt. Erebus, Antarctica) were investigated by single-crystal X-ray diffraction combined with electron probe microanalysis which together provide accurate site occupancy and site configuration parameters. Variations in site volumes distinguish the clinopyroxenes belonging to the more alkaline B-Ph suite from those of the AB-T suite. The former have higher V_{M2} and, for similar cell volume, lower V_{M1} and higher V_T. In these *C2/c* pyroxenes, the bond lengths of *M*1 depend on R^{3+} content, necessary to balance Al^{IV} in the *T* site. *M*1 geometric variations are similar for both B-Ph and AB-T suites. However, the *M*2 site is crucial for variations in polyhedral configurations. The increase in Al^{IV} affects the shortest *M*2–O bond lengths in different ways depending on (Ca+Na) contents in the *M*2 site. Thus, the clinopyroxenes were distinguished in two different groups not related to the two suites. The first group is characterized by (Ca+Na) higher than 0.90 atoms per formula unit but shows a good positive correlation between the shortest *M*2–O bond lengths and Al^{IV} content, at quite constant (Ca+Na). The second group has (Ca+Na) less than 0.90 atoms per formula unit but shows a poor correlation between the shortest *M*2–O bond lengths and Al^{IV} content. In general, shortening of the longest *M*2–O bond lengths is associated with increase in Al^{IV}. The cell and *M*1 volumes suggest that the clinopyroxenes, including the larger and sometimes resorbed macrocrysts, crystallized at a pressure lower than 5 kbar, fitting the petrography and evolved character of the rocks in question.

KEYWORDS: clinopyroxene, X-ray diffraction, site occupancy, Antarctica.

Introduction

CRYSTAL chemical study of several *C2/c* pyroxenes (cpx) based on single-crystal X-ray diffraction and microanalysis techniques on the same crystal has been carried out in the last few years. Dal Negro *et al.* (1989) summarized crystal chemical variations in cpx from distinct magmatic environments and

Mineralogical Magazine, April 1997, Vol. 61, pp. 423–439

stressed the fact that cpx is a sensitive genetic indicator related to specific host rocks. Its structural geometry depends on the various cation occupancies in the *M*1, *M*2 and *T* sites, as well as the relationships between the sites, and the charge balance around the oxygens, the latter being obtained by means of cation-oxygen bond length variations.

The present work evaluates similarities and differences in the crystal chemistry of cpx from sodic volcanic rocks from suites with various degrees of silica-undersaturation (see below). Moreover, the pressure of cpx crystallization, including that of the larger and sometimes corroded cpx macrocrysts, is estimated. The volcanics mainly come from the Mt. Melbourne Province (McMurdo Volcanic Group, Western Ross Embayment, Antarctica).

Geological setting and petrological outlines

The Mt. Melbourne Volcanic Province (MMVP) is part of the McMurdo Volcanic Group which comprises all Cenozoic alkaline volcanic rocks outcropping in the Western Ross Embayment in Antarctica (Kyle, 1990). The MMVP extends northward from Mt. Melbourne to the Malta Plateau (Fig. 1), on the uplifted western shoulder of the Ross

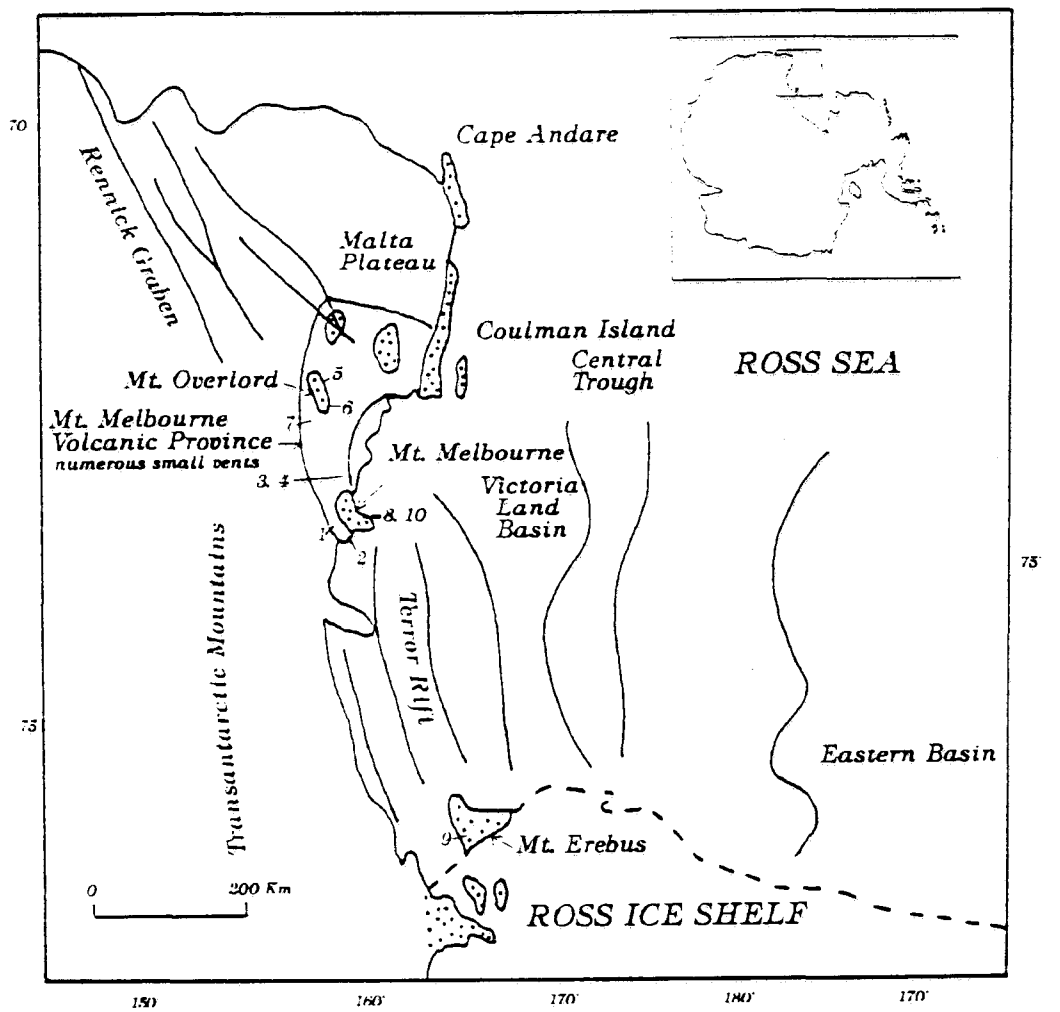

FIG. 1. Schematic tectonic map of western Ross Sea Rift (modified after Kyle, 1990), showing sites of analysed samples (1 to 10) reported in Table 1. Dotted areas: distribution of McMurdo Volcanic Group.

Sea Rift System. The age of the MMVP volcanism is younger than 25 Ma, Late Oligocene to Quaternary (Kyle, 1990). The investigated samples (0.1–8 Ma; Kyle, 1990) belong to various volcanic centres and represent scoriae, bombs and lava flows. They are located mainly south and east of Mt. Melbourne and south of Mt. Overlord (Fig. 1).

The MMVP volcanics are mostly represented by sodic alkaline rocks (20–1% CIPW nepheline); hypersthene- and quartz-normative rocks are volumetrically scarce. The R1–R2 classification of De La Roche *et al.* (1980) (Fig. 2) shows that these rocks (Table 1) belong to two main suites: Basanite-Phonolite (B-Ph) and the less alkaline Alkali basalt-Trachyphonolite (AB-T) (see also Table 1 and Antonini *et al.*, 1994).

The B-Ph rocks show olivine and augite with a porphyritic texture and abundant vesicles; kaersutitic amphibole is an important phenocryst phase only in phonotephrite (no. 9); plagioclase is confined to the groundmass. Basanite (no. 6) is characterized by the presence of spinel-lherzolite mantle nodules. The rocks of the AB-T suite have subaphyric to strongly porphyritic texture. In contrast with the B-Ph suite, plagioclase is an important phenocryst phase even in the least evolved rocks (mg#, less than 48; Table 1), associated with olivine and clinopyroxene.

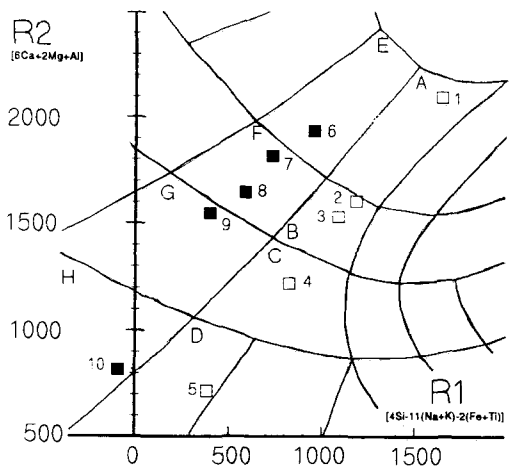

FIG. 2. Classification diagram of De La Roche *et al.* (1980) showing that the studied rocks may be subdivided into basanitic-phonolite (B-Ph, filled squares) and alkali basalt-trachyte (AB-T, open squares) suites. A = alkali-basalt; B = hawaiite; C = mugearite; D = trachyphonolite; E = basanite; F = tephrite; G = phonotephrite; H = phonolite. Numbers 1 to 10 refer to rock types reported in Table 1.

Major and trace element chemistry (Table 1) shows that there is some compositional overlap (e.g. SiO_2, Al_2O_3, TiO_2, CaO) between the B-Ph and AB-T suites. However, the B-Ph rocks have higher alkali and incompatible trace element contents than with those of the AB-T rocks. Basanite (no. 6) is characterized by higher *LREE/HREE* ratios (e.g. La_N/Yb_N = 18.3) than those of alkali-basalt (no. 1; La_N/Yb_N = 14.5), according to Antonini *et al.* (1994). Notably, mg# *vs.* Na_2O, K_2O, La, Zr and Y (Table 1) show similar but distinct trends in the two suites.

Mass balance calculations (Antonini *et al.*, 1994) indicate that the transition basanite-tephrite-phonotephrite-phonolite (B-Ph suite) is compatible with fractional crystallization involving olivine, clinopyroxene, and minor magnetite, apatite and amphibole. The transition alkali basalt-hawaiite-mugearite-trachyphonolite (AB-T suite) is compatible with gabbro fractionation involving olivine, clinopyroxene, plagioclase, and minor magnetite and apatite.

In summary, petrographic, geochemical and mass balance data suggest that both B-Ph and AB-T suites evolved by fractional crystallization from parental melts corresponding to basanite and alkali-basalt, respectively.

Analytical procedures

Optically homogeneous crystal fragments (about 0.2 mm in diameter) were hand-picked from a section about 100 μm thick for X-ray diffraction and microanalysis. They usually come from the core and rim of a single phenocryst, and some from a single microphenocryst.

X-ray diffraction data were recorded on an automated SIEMENS AED II diffractometer using Mo-$K\alpha$ radiation monochromatized by a flat graphite crystal, using the techniques and procedures given in Dal Negro *et al.* (1982).

The same crystals used for X-ray single-crystal analysis were used for chemical analyses, performed on a CAMECA-CAMEBAX microprobe operating at 15 kV and 15 nA. A PAP CAMECA program was used to convert X-ray counts into weight percent of the corresponding oxides. Results are considered accurate to within 2–3% for major and 10% for minor elements.

Site occupancies were calculated according to Dal Negro *et al.* (1982). The calculation of Fe^{3+} is based both on charge balance (Papike *et al.*, 1974) and geometric parameters. The mean of *M*1–O bond lengths derived from crystal structure refinement ($<M1-O>_{obs}$) was compared with that calculated from the site occupancies of the various cations, on the basis of the following equation:

TABLE 1. Whole rock analyses of major (wt.%) and trace (ppm) elements for the studied rocks. Data were acquired by means of a PW 1404 XRF spectrometer, using the PH model of X40 Philips Software (v. 4.C; Philips, 1994) for the matrix effects correction. mg#= [Mg/(Mg+Fe^{2+})]X100 assuming $Fe_2O_3/FeO = 0.20$

	Alkali basalt-trachyphonolite (AB-T) suite					Basanite-phonolite (B-Ph) suite				
Sample	VG3015	VG3106	VG3150	VG3151	VG3187F	VG3243	VG3022	VG3314	VG3276	VG3185
	no.1	no. 2	no. 3	no. 4	no. 5	no. 6	no. 7	no. 8	no. 9	no. 10
Rocktype	Alkali-basalt	Hawaiite	Hawaiite	Mugearite	Trachy-phonolite	Basanite	Tephrite	Tephrite	Phono-tephrite	Phonolite
SiO_2 (wt.%)	46.01	46.53	47.68	52.48	60.00	44.38	44.52	44.66	46.25	56.88
TiO_2	2.62	3.73	3.12	2.22	0.99	3.41	4.03	3.87	3.64	1.11
Al_2O_3	13.55	17.09	17.58	17.28	18.27	13.54	14.48	15.61	14.80	18.41
FeO_{tot}	11.45	12.64	12.29	9.99	5.23	12.36	11.83	12.67	12.00	6.72
MnO	0.17	0.18	0.22	0.21	0.15	0.20	0.19	0.19	0.20	0.20
MgO	10.34	5.56	3.37	2.59	1.02	9.30	8.18	6.07	6.87	1.22
CaO	12.30	9.27	9.49	7.02	2.86	11.24	10.51	9.70	8.52	3.70
Na_2O	2.50	3.55	3.75	4.95	6.85	3.40	3.97	4.30	4.91	7.57
K_2O	0.63	0.90	1.44	2.49	4.31	1.56	1.68	1.75	2.21	3.84
P_2O_5	0.42	0.54	1.05	0.77	0.32	0.62	0.61	1.18	0.60	0.35
mg#	65.5	48.0	36.6	35.3	29.1	61.3	59.2	50.2	54.6	27.6
Ne (CIPW)	7.40	4.61	3.48	3.95	3.27	14.94	15.84	13.86	17.22	13.10
Cr (ppm)	572	73	52	80	3	279	247	165	109	17
Ni	206	52	31	34	10	176	113	123	120	11
Ba	196	283	748	1253	963	420	481	397	547	929
Rb	15	22	23	40	132	32	33	39	59	116
Sr	564	792	919	615	508	722	929	958	1067	481
Zr	132	163	184	200	658	246	202	353	461	815
Y	19	29	37	26	42	37	36	46	45	66
Nb	37	52	59	85	110	95	84	95	141	214
La	28	34	52	56	126	57	58	56	78	150
Ce	52	69	98	108	215	117	108	130	144	248
Nd	26	35	48	51	77	62	54	58	68	100

$$2.081\ Mg_{M1} + 2.126Fe^{2+}_{M1} + 2.030Fe^{3+} + 1.930Al^{VI} + 2.010Cr^{3+} + 1.990Ti^{4+} = <M1-O>_{calc}$$

where 2.081, 2.126, 2.030, 1.930, 2.010 and 1.990 are the means of $M1-O$ bond lengths in the octahedrons coordinated by Mg, Fe^{2+}, Fe^{3+}, Al^{VI}, Cr^{3+} and Ti^{4+}, respectively (Shannon, 1976). When the $|<M1-O>_{obs} - <M1-O>_{calc}|$ difference was lower than 0.0050 Å, the $(Fe^{2+}/Fe^{3+})_{M1}$ ratio was modified according to Secco (1988). In the investigated cpx, the maximum $<M1-O>$ difference was 0.005 Å (one crystal; mean 0.002 ± 0.002 Å, N = 29).

Chemical and crystallographic data are reported in Tables 2 and 3, respectively; bond lengths and volume data are reported in Table 4.

Crystal chemistry

In the conventional pyroxene quadrilateral Ca-Mg-Fe_t (Fe^{2+} + Fe^{3+} + Mn), the studied cpx (Table 2) fall in the diopside and augite fields (Fig. 3).

M1 site. The $M1$ site is essentially filled by Mg (0.62–0.74 a.f.u.: atoms per formula unit), except for crystal 8 of hawaiite no. 3 which is characterized by an Mg content of 0.82 a.f.u.. Fe^{2+} ranges from 0.06 to 0.30 a.f.u. and R^{3+} (Al^{VI} + Fe^{3+} + Cr^{3+} + Ti^{4+}) from 0.05 to 0.24 a.f.u., without distinction between B-Ph and AB-T cpx (Table 2).

The volume of the quite regular $M1$ octahedron (V_{M1}) increases from 11.5 to 12.1 $Å^3$ (Table 4), with decreasing R^{3+} content. The V_{M1} increase is due to lengthening of all $M1-O$ bond lengths; the lengthening of the shortest $M1-O2$ bond lengths (2.009–2.057 Å) shows the best relationship with the R^{3+} decrease.

T site. In the tetrahedral site, Al^{IV} contents range from 0.02 to 0.25 a.f.u. (Table 2). The Al^{IV} increase is poorly correlated with the increase in tetrahedral volume (V_T = 2.23–2.29 $Å^3$; Table 4). Note that for similar Al^{IV} contents, V_T may have different values. Actually, the crystals from the B-Ph suite have a larger V_T, except for crystals 24 and 25 of phonotephrite (no. 9), and 27 and 29 of phonolite (no. 10).

M2 site. The crystals of the AB-T suite have (Ca+Na) lower than 0.89 a.f.u., excluding crystals 15 and 16 of trachyphonolite (no. 5). In the B-Ph suite, the cpx (Ca+Na) is higher than 0.90 a.f.u., except for crystals 24, 25 and 26 of phonotephrite (no. 9), and 22 and 23 of tephrite no. 8 (Table 2, Fig. 4).

The volume of the $M2$ polyhedron (V_{M2}) ranges from 25.38 to 25.87 $Å^3$ (Table 4) and generally increases with (Ca+Na) content. Note that the

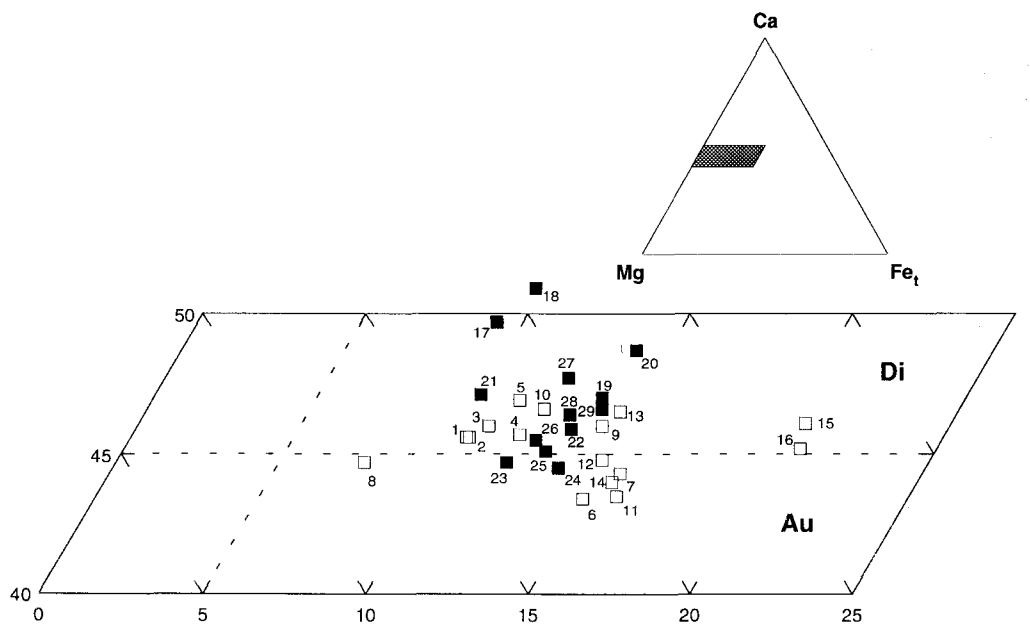

FIG. 3. AB-T and B-Ph clinopyroxene compositions projected in Ca-Mg-Fe_t (Fe^{2+}+Fe^{3+}+Mn) system. Symbols as in Fig. 2.

TABLE 2. Chemical compositions and site occupancies for cpx of AB-T and B-Ph suites. M, P and gm: macrocrysts, phenocrysts and groundmass crystals, respectively; c and r: core and rim, respectively. AB-T suite: 1–5 = alkali basalt; 6–10 = hawaiite; 11–14 = mugearite; 15–16 = trachyphonolite. B-Ph suite: 17–18 = basanite; 19–23 = tephrite; 24–26 = phonotephrite; 27–29 = phonolite

AB-T suite	VG3015					VG3106		VG3150			VG3151				VG3187	
	1	2	3	4	5	6	7	8	9	10	11	12	13	14	15	16
	M c	M r	P c	P r	gm	M c	P c	M r	P r	gm	M c	M r	P c	P r	P c	P r
SiO_2	49.18	49.33	48.58	48.21	47.84	47.86	48.36	52.37	47.05	47.65	49.61	49.67	47.48	48.91	52.30	52.10
TiO_2	1.27	1.20	1.50	1.80	1.69	2.24	1.80	0.76	2.33	1.63	1.59	1.55	2.33	1.64	0.51	0.40
Al_2O_3	6.63	6.56	6.80	8.24	7.39	6.75	6.13	3.68	7.48	7.11	4.73	5.23	7.12	4.84	1.11	1.20
FeO	4.73	4.60	4.29	5.10	3.99	6.57	6.87	3.98	5.07	4.36	7.76	7.21	6.44	5.94	11.18	11.86
Fe_2O_3	1.53	1.57	2.24	1.85	2.80	2.28	2.21	0.66	3.59	3.00	1.70	1.60	2.06	3.50	1.16	0.13
MgO	14.61	14.57	14.28	13.77	13.76	13.63	13.04	16.56	13.05	13.57	13.50	13.35	12.60	13.66	11.59	13.00
MnO	0.07	0.13	0.10	0.13	0.13	0.14	0.26	0.12	0.06	0.12	0.31	0.21	0.18	0.27	0.47	0.61
CaO	21.09	21.04	21.15	20.67	21.49	19.76	20.12	21.58	21.04	21.32	20.20	20.69	20.97	20.67	22.25	21.32
Na_2O	0.45	0.52	0.54	0.65	0.55	0.63	0.71	0.44	0.65	0.53	0.59	0.66	0.63	0.63	0.47	0.50
Cr_2O_3	0.29	0.12	0.33	0.01	0.34	0.11	0.00	0.59	0.00	0.09	0.02	0.00	0.02	0.02	0.00	0.02
Total	99.85	99.64	99.81	100.43	99.98	99.97	99.50	100.74	100.32	99.38	100.01	100.17	99.83	100.08	101.04	101.14
T site																
Si	1.812	1.819	1.794	1.769	1.768	1.779	1.809	1.899	1.745	1.774	1.849	1.844	1.771	1.821	1.962	1.978
Al^{IV}	0.188	0.181	0.206	0.231	0.232	0.221	0.191	0.101	0.255	0.226	0.151	0.156	0.229	0.179	0.038	0.022
Σ	2.000	2.000	2.000	2.000	2.000	2.000	2.000	2.000	2.000	2.000	2.000	2.000	2.000	2.000	2.000	2.000
*M*1 site																
Al^{VI}	0.099	0.104	0.090	0.126	0.090	0.075	0.079	0.056	0.072	0.086	0.057	0.073	0.084	0.034	0.011	0.032
Fe^{2+}	0.089	0.125	0.110	0.097	0.077	0.094	0.159	0.072	0.103	0.104	0.141	0.163	0.151	0.108	0.294	0.304
Fe^{3+}	0.042	0.013	0.032	0.051	0.078	0.084	0.032	0.018	0.080	0.054	0.048	0.025	0.028	0.098	0.033	0.004
Mg	0.727	0.722	0.716	0.676	0.698	0.681	0.679	0.816	0.680	0.707	0.708	0.696	0.671	0.713	0.648	0.648
Cr^{3+}	0.008	0.003	0.010	0.000	0.010	0.003	0.000	0.017	0.000	0.003	0.001	0.000	0.001	0.001	0.000	0.001
Ti^{4+}	0.035	0.033	0.042	0.050	0.047	0.063	0.051	0.021	0.065	0.046	0.045	0.043	0.065	0.046	0.014	0.011
Σ	1.000	1.000	1.000	1.000	1.000	1.000	1.000	1.000	1.000	1.000	1.000	1.000	1.000	1.000	1.000	1.000
R^{3+}[1]	0.184	0.153	0.174	0.227	0.225	0.225	0.162	0.112	0.217	0.189	0.151	0.141	0.178	0.179	0.058	0.048
M2 site																
Ca	0.832	0.831	0.837	0.813	0.851	0.787	0.806	0.838	0.836	0.851	0.807	0.823	0.838	0.825	0.894	0.867
Na	0.032	0.037	0.039	0.046	0.039	0.045	0.051	0.031	0.047	0.038	0.043	0.048	0.046	0.045	0.034	0.037
Mg	0.077	0.081	0.070	0.078	0.060	0.074	0.049	0.079	0.041	0.046	0.042	0.043	0.030	0.045	0.000	0.004
Fe^{2+}	0.057	0.047	0.051	0.059	0.046	0.090	0.086	0.048	0.074	0.061	0.098	0.079	0.080	0.076	0.057	0.072
Mn	0.002	0.004	0.003	0.004	0.004	0.004	0.008	0.004	0.002	0.004	0.010	0.007	0.006	0.009	0.015	0.020
Σ	1.000	1.000	1.000	1.000	1.000	1.000	1.000	1.000	1.000	1.000	1.000	1.000	1.000	1.000	1.000	1.000
Ca+Na	0.864	0.868	0.876	0.859	0.890	0.832	0.857	0.869	0.883	0.889	0.850	0.871	0.884	0.870	0.928	0.904

[1] $R^{3+} = (Al^{VI} + Fe^{3+} + Cr^{3+} + Ti^{4+})$

TABLE 2. (*contd*)

B-Ph suite	VG3243		VG3022			VG3314		VG3276			VG3185		
	17	18	19	20	21	22	23	24	25	26	27	28	29
	P c	P c	P c	P r	gm	P c	gm	P c	P r	gm	M r	P c	P r
SiO_2	47.37	49.02	47.28	47.40	48.04	48.46	49.00	48.66	48.81	47.76	48.53	51.46	50.80
TiO_2	2.88	2.58	2.54	2.57	2.16	2.22	1.91	1.83	1.62	2.52	2.36	1.40	1.47
Al_2O_3	6.33	4.92	7.61	8.03	6.73	6.03	5.81	7.14	6.63	8.38	5.97	1.40	3.17
FeO	1.94	4.19	6.76	7.68	4.47	5.70	5.50	6.82	5.20	5.76	6.80	6.37	8.01
Fe_2O_3	3.66	1.72	1.07	0.11	1.76	2.22	1.65	0.79	2.33	1.37	0.39	1.36	0.14
MgO	13.76	13.15	12.65	11.78	14.03	13.36	14.40	13.14	13.28	13.32	13.23	13.65	13.37
MnO	0.27	0.13	0.16	0.13	0.06	0.16	0.13	0.16	0.06	0.03	0.16	0.25	0.28
CaO	23.16	23.68	21.10	21.40	21.62	20.98	20.69	19.46	19.91	20.07	22.00	21.74	21.99
Na_2O	0.60	0.62	0.78	0.80	0.60	0.69	0.61	1.18	1.16	0.74	0.51	0.72	0.72
Cr_2O_3	0.03	0.00	0.03	0.10	0.51	0.17	0.27	0.82	0.99	0.03	0.03	0.00	0.03
Total	100.00	100.01	99.98	99.49	99.98	99.99	99.97	100.00	99.99	99.98	99.98	98.35	99.98
T site													
Si	1.752	1.818	1.755	1.763	1.773	1.800	1.810	1.799	1.805	1.765	1.801	1.911	1.888
Al^{IV}	0.248	0.182	0.245	0.237	0.227	0.200	0.190	0.201	0.195	0.235	0.199	0.089	0.112
Σ	2.000	2.000	2.000	2.000	2.000	2.000	2.000	2.000	2.000	2.000	2.000	2.000	2.000
M1 site													
Al^{VI}	0.028	0.033	0.088	0.115	0.066	0.064	0.063	0.110	0.094	0.130	0.062	0.044	0.027
Fe^{2+}	0.060	0.130	0.126	0.184	0.084	0.099	0.086	0.130	0.090	0.105	0.167	0.155	0.213
Fe^{3+}	0.102	0.048	0.030	0.003	0.049	0.062	0.046	0.022	0.065	0.038	0.011	0.038	0.004
Mg	0.729	0.716	0.684	0.623	0.726	0.708	0.744	0.663	0.677	0.656	0.693	0.724	0.714
Cr^{3+}	0.001	0.000	0.001	0.003	0.015	0.005	0.008	0.024	0.029	0.001	0.001	0.000	0.001
Ti^{4+}	0.080	0.072	0.071	0.072	0.060	0.062	0.053	0.051	0.045	0.070	0.066	0.039	0.041
Σ	1.000	0.999	1.000	1.000	1.000	1.000	1.000	1.000	1.000	1.000	1.000	1.000	1.000
$R^{3+[1]}$	0.211	0.153	0.190	0.193	0.190	0.193	0.170	0.207	0.233	0.239	0.140	0.121	0.073
M2 site													
Ca	0.919	0.941	0.839	0.853	0.855	0.835	0.819	0.771	0.789	0.795	0.875	0.865	0.876
Na	0.043	0.044	0.056	0.058	0.043	0.050	0.044	0.084	0.083	0.053	0.037	0.052	0.052
Mg	0.030	0.011	0.016	0.030	0.054	0.032	0.049	0.060	0.055	0.078	0.039	0.032	0.027
Fe^{2+}	0.000	0.000	0.084	0.055	0.045	0.078	0.084	0.080	0.071	0.073	0.044	0.043	0.036
Mn	0.008	0.004	0.005	0.004	0.003	0.005	0.004	0.005	0.002	0.001	0.005	0.008	0.009
Σ	1.000	1.000	1.000	1.000	.100	1.000	1.000	1.000	1.000	1.000	1.000	1.000	1.000
Ca+Na	0.962	0.985	0.895	0.911	0.898	0.885	0.863	0.855	0.872	0.848	0.912	0.917	0.928

[1] $R^{3+} = (Al^{VI} + Fe^{3+} + Cr^{3+} + Ti^{4+})$

TABLE 3. Crystallographic data for cpx of AB-T and B-Ph suites. Standard deviations in brackets. Other abbreviations as in Table 2

AB-T suite		VG3015					VG3106		VG3150			VG3151				VG3187	
		1	2	3	4	5	6	7	8	9	10	11	12	13	14	15	16
		Mc	Mr	Pc	Pr	gm	Mc	Pc	Mr	Pr	gm	Mc	Mr	Pc	Pr	Pc	Pr
	a (Å)	9.736 [1]	9.734 [1]	9.738 [1]	9.724 [1]	9.733 [1]	9.734 [1]	9.745 [1]	9.734 [1]	9.738 [1]	9.743 [1]	9.743 [1]	9.748 [1]	9.739 [1]	9.750 [1]	9.764 [1]	9.772 [1]
	b (Å)	8.882 [2]	8.882 [1]	8.882 [2]	8.865 [1]	8.874 [2]	8.875 [1]	8.892 [2]	8.898 [2]	8.875 [2]	8.882 [2]	8.897 [2]	8.898 [2]	8.881 [2]	8.897 [2]	8.943 [2]	8.949 [2]
	c (Å)	5.280 [1]	5.278 [1]	5.282 [1]	5.278 [1]	5.279 [1]	5.281 [1]	5.282 [1]	5.264 [1]	5.282 [1]	5.284 [1]	5.274 [1]	5.280 [1]	5.278 [1]	5.283 [1]	5.260 [1]	5.264 [1]
	β °	106.25 [1]	106.27 [1]	106.23 [1]	106.33 [1]	106.23 [1]	106.29 [1]	106.29 [1]	106.23 [1]	106.22 [1]	106.22 [1]	106.19 [1]	106.20 [1]	106.20 [1]	106.18 [1]	105.91 [1]	105.91 [1]
	V_{cell} (Å^3)	438.35	438.10	438.68	436.62	437.77	437.92	439.34	437.80	438.37	439.08	439.02	439.87	438.37	440.09	441.70	442.68
	N ref $_{obs}$	517	502	547	470	542	538	554	499	508	522	543	525	518	483	475	600
	R_{obs}(%)	2.40	2.76	2.26	2.59	2.01	2.10	1.99	2.43	2.29	2.34	2.16	2.23	2.33	2.34	2.58	2.01
M1	Mg occ	0.852 [2]	0.860 [2]	0.854 [2]	0.838 [2]	0.836 [2]	0.800 [2]	0.796 [2]	0.906 [1]	0.800 [2]	0.820 [2]	0.794 [2]	0.798 [2]	0.804 [2]	0.790 [2]	0.692 [2]	0.688 [2]
	y	0.9067 [1]	0.9070 [1]	0.9069 [1]	0.9066 [1]	0.9068 [1]	0.9064 [1]	0.9065 [1]	0.9074 [1]	0.9066 [1]	0.9066 [1]	0.9065 [1]	0.9066 [1]	0.9065 [1]	0.9066 [1]	0.9071 [1]	0.9069 [1]
	Beq	0.53 [3]	0.52 [3]	0.54 [2]	0.55 [2]	0.50 [2]	0.52 [2]	0.50 [2]	0.48 [3]	0.53 [3]	0.53 [2]	0.54 [2]	0.61 [2]	0.50 [2]	0.60 [3]	0.57 [2]	0.52 [3]
M2	Ca occ	0.904 [4]	0.880 [5]	0.892 [4]	0.880 [5]	0.904 [4]	0.906 [4]	0.918 [4]	0.874 [5]	0.914 [4]	0.820 [2]	0.944 [4]	0.926 [4]	0.904 [4]	0.928 [4]	0.992 [2]	0.992 [1]
	y	0.2997 [1]	0.2993 [1]	0.3001 [1]	0.2996 [1]	0.3001 [1]	0.2996 [1]	0.2998 [1]	0.2988 [1]	0.3000 [1]	0.2998 [1]	0.2987 [1]	0.2991 [1]	0.2997 [1]	0.2992 [1]	0.2985 [1]	0.2986 [1]
	Beq	0.76 [3]	0.89 [3]	1.01 [1]	0.97 [3]	0.96 [2]	1.01 [2]	1.04 [2]	0.87 [2]	0.53 [3]	1.01 [2]	1.03 [2]	1.07 [2]	1.04 [2]	1.07 [2]	0.91 [2]	0.99 [2]
T	x	0.2881 [1]	0.2881 [1]	0.2880 [1]	0.2883 [1]	0.2881 [1]	0.2884 [1]	0.2883 [1]	0.2880 [1]	0.2882 [1]	0.2882 [1]	0.2881 [1]	0.2881 [1]	0.2881 [1]	0.2882 [1]	0.2876 [1]	0.2876 [1]
	y	0.0929 [1]	0.0930 [1]	0.0930 [1]	0.0931 [1]	0.0930 [1]	0.0928 [1]	0.0927 [1]	0.0929 [1]	0.0927 [1]	0.0928 [1]	0.0927 [1]	0.0927 [1]	0.0929 [1]	0.0927 [1]	0.0925 [1]	0.0926 [1]
	z	0.2306 [1]	0.2310 [1]	0.2304 [1]	0.2308 [1]	0.2302 [1]	0.2308 [1]	0.2315 [1]	0.2319 [1]	0.2306 [1]	0.2303 [1]	0.2315 [1]	0.2312 [1]	0.2306 [1]	0.2311 [1]	0.2323 [1]	0.2321 [1]
	Beq	0.59 [1]	0.61 [2]	0.62 [1]	0.58 [2]	0.57 [1]	0.58 [1]	0.57 [1]	0.58 [2]	0.50 [1]	0.60 [1]	0.58 [1]	0.65 [1]	0.58 [1]	0.65 [2]	0.50 [2]	0.55 [1]
O1	x	0.1147 [1]	0.1147 [2]	0.1145 [1]	0.1143 [2]	0.1145 [1]	0.1145 [1]	0.1152 [1]	0.1154 [1]	0.1146 [4]	0.1146 [1]	0.1153 [1]	0.1150 [1]	0.1147 [1]	0.1150 [1]	0.1168 [2]	0.1167 [1]
	y	0.0870 [2]	0.0868 [2]	0.0869 [1]	0.0867 [2]	0.0868 [1]	0.0868 [1]	0.0870 [1]	0.0872 [2]	0.0868 [2]	0.0869 [1]	0.0872 [1]	0.0870 [1]	0.0870 [2]	0.0872 [2]	0.0876 [2]	0.0878 [1]
	z	0.1398 [3]	0.1403 [3]	0.1400 [3]	0.1396 [3]	0.1397 [2]	0.1396 [3]	0.1407 [2]	0.1412 [3]	0.1396 [3]	0.1400 [3]	0.1414 [3]	0.1412 [3]	0.1398 [3]	0.1409 [3]	0.1442 [3]	0.1443 [2]
	Beq	0.80 [3]	0.80 [3]	0.81 [3]	0.77 [3]	0.76 [2]	0.77 [3]	0.77 [2]	0.75 [3]	0.64 [3]	0.81 [3]	0.73 [3]	0.81 [3]	0.77 [3]	0.84 [3]	0.67 [3]	0.72 [2]
O2	x	0.3632 [2]	0.3632 [2]	0.3630 [1]	0.3635 [2]	0.3631 [1]	0.3632 [2]	0.3634 [1]	0.3629 [2]	0.3631 [2]	0.3634 [1]	0.3632 [1]	0.3633 [2]	0.3632 [2]	0.3632 [2]	0.3624 [2]	0.3624 [1]
	y	0.2521 [2]	0.2515 [2]	0.2521 [1]	0.2523 [2]	0.2523 [1]	0.2523 [2]	0.2518 [1]	0.2506 [2]	0.2523 [2]	0.2520 [2]	0.2512 [1]	0.2514 [2]	0.2521 [2]	0.2516 [2]	0.2489 [2]	0.2493 [1]
	z	0.3226 [3]	0.3229 [3]	0.3223 [3]	0.3230 [3]	0.3227 [3]	0.3232 [3]	0.3234 [3]	0.3231 [3]	0.3226 [2]	0.3228 [3]	0.3236 [3]	0.3230 [3]	0.3226 [3]	0.3230 [3]	0.3225 [4]	0.3225 [2]
	Beq	1.07 [3]	1.08 [3]	1.12 [3]	1.06 [1]	1.05 [3]	1.06 [3]	1.07 [3]	1.06 [3]	0.98 [3]	1.06 [3]	1.08 [3]	1.14 [3]	1.07 [3]	1.15 [3]	0.93 [4]	0.95 [2]
O3	x	0.3518 [1]	0.3516 [2]	0.3517 [1]	0.3517 [2]	0.3519 [1]	0.3518 [1]	0.3518 [1]	0.3511 [1]	0.3519 [1]	0.3517 [1]	0.3515 [1]	0.3516 [1]	0.3518 [1]	0.3515 [1]	0.3508 [2]	0.3508 [1]
	y	0.0188 [2]	0.0190 [2]	0.0189 [1]	0.0189 [2]	0.0191 [1]	0.0190 [2]	0.0190 [1]	0.0191 [2]	0.0188 [2]	0.0190 [1]	0.0190 [1]	0.0190 [2]	0.0188 [2]	0.0191 [2]	0.0186 [2]	0.0186 [1]
	z	−0.0038 [3]	−0.0042 [3]	−0.0043 [3]	−0.0041 [3]	−0.0048 [2]	−0.0041 [3]	−0.0034 [2]	−0.0039 [3]	−0.0049 [3]	−0.0046 [3]	−0.0035 [3]	−0.0039 [3]	−0.0038 [3]	−0.0043 [3]	−0.0039 [3]	0.0034 [2]
	Beq	0.90 [3]	0.93 [4]	0.94 [3]	0.88 [3]	0.90 [3]	0.96 [3]	0.92 [3]	0.91 [3]	0.74 [3]	0.89 [3]	0.84 [3]	0.95 [3]	0.86 [3]	0.97 [3]	0.70 [3]	0.77 [2]
M2'	Fe occ	0.007 [7]	0.009 [9]	0.009 [7]	0.009 [9]	0.007 [6]	0.009 [7]	0.010 [7]	0.010 [8]	0.011 [8]	0.007 [8]	0.009 [7]	0.009 [8]	0.007 [7]	0.009 [8]	0.008 [9]	0.008 [6]
	y	0.2220	0.2223	0.2221	0.2225	0.2218	0.2219	0.2218	0.2222	0.2224	0.2222	0.2218	0.2218	0.2220	0.2223	0.2229	0.2219
	Beq	1.06	1.07	1.07	1.05	1.02	1.08	1.12	1.05	0.97	1.05	1.10	1.14	1.10	1.14	0.95	1.03

TABLE 3 (*contd*)

B-Ph suite		VG3243		VG3022			VG3314		VG3276			VG3185		
		17	18	19	20	21	22	23	24	25	26	27	28	29
		Pc	Pc	Pc	Pr	gm	Pc	gm	Pc	Pr	gm	Mr	Pc	Pr
	a (Å)	9.765 [1]	9.764 [1]	9.747 [1]	9.754 [1]	9.749 [1]	9.746 [1]	9.749 [1]	9.731 [1]	9.731 [1]	9.735 [1]	9.756 [1]	9.759 [1]	9.764 [1]
	b (Å)	8.896 [3]	8.902 [2]	8.883 [2]	8.884 [2]	8.888 [3]	8.885 [2]	8.889 [2]	8.879 [2]	8.875 [2]	8.864 [2]	8.903 [2]	8.911 [2]	8.931 [2]
	c (Å)	5.294 [1]	5.289 [1]	5.288 [1]	5.294 [1]	5.289 [1]	5.287 [1]	5.285 [1]	5.280 [1]	5.282 [1]	5.291 [1]	5.283 [1]	5.279 [1]	5.273 [1]
	β °	105.91 [1]	105.94 [1]	106.15 [1]	106.09 [1]	106.14 [1]	106.21 [1]	106.17 [1]	106.28 [1]	106.30 [1]	106.27 [1]	106.06 [1]	106.10 [1]	105.98 [1]
	V_{cell} (Å^3)	442.27	442.04	439.78	440.78	440.02	439.62	439.87	437.91	437.83	438.28	441.00	441.07	442.05
	N ref $_{obs}$	454	571	571	591	522	561	542	561	513	514	566	520	556
	R_{obs}(%)	2.74	1.92	2.00	1.75	2.19	2.10	1.93	1.81	1.97	2.26	1.93	2.16	2.03
*M*1	Mg occ	0.798 [2]	0.802 [2]	0.790 [2]	0.778 [2]	0.830 [2]	0.808 [2]	0.814 [2]	0.804 [2]	0.802 [2]	0.820 [2]	0.792 [2]	0.806 [2]	0.764 [2]
	y	0.9069 [1]	0.9069 [1]	0.9064 [1]	0.9064 [1]	0.9066 [1]	0.9064 [1]	0.9066 [1]	0.9065 [1]	0.9064 [1]	0.9063 [1]	0.9068 [1]	0.9068 [1]	0.9069 [1]
	Beq	0.50 [2]	0.60 [2]	0.59 [2]	0.56 [2]	0.52 [2]	0.59 [2]	0.57 [2]	0.58 [2]	0.58 [2]	0.58 [2]	0.59 [2]	0.58 [2]	0.59 [2]
M2	Ca occ	0.922 [5]	0.930 [3]	0.920 [4]	0.900 [4]	0.916 [4]	0.930 [4]	0.928 [4]	0.694 22	0.876 [4]	0.882 [4]	0.930 [4]	0.920 [4]	0.902 [4]
	y	0.3029 [1]	0.3025 [1]	0.3010 [1]	0.3020 [1]	0.3012 [1]	0.3000 [1]	0.3001 [1]	0.3017 [4]	0.2999 [1]	0.3009 [1]	0.3009 [1]	0.2999 [2]	0.3002 [1]
	Beq	0.79 [1]	0.91 [2]	1.02 [2]	0.93 [2]	0.95 [2]	1.09 [2]	1.04 [2]	0.80 [6]	1.08 [2]	1.06 [2]	0.99 [2]	11.84 [1]	0.92 [2]
T	x	0.2817 [1]	0.2870 [1]	0.2879 [1]	0.2878 [1]	0.2879 [1]	0.2881 [1]	0.2880 [1]	0.2882 [1]	0.2882 [1]	0.2883 [1]	0.2876 [1]	0.2877 [1]	0.2874 [1]
	y	0.0932 [1]	0.0932 [1]	0.0928 [1]	0.0929 [1]	0.0930 [1]	0.0927 [1]	0.0928 [1]	0.0927 [1]	0.0928 [1]	0.0930 [1]	0.0930 [1]	0.0930 [1]	0.0928 [1]
	z	0.2278 [1]	0.2285 [1]	0.2297 [1]	0.2292 [1]	0.2297 [1]	0.2305 [1]	0.2304 [1]	0.2307 [1]	0.2306 [1]	0.2298 [1]	0.2299 [1]	0.2307 [1]	0.2310 [1]
	Beq	0.55 [2]	0.60 [1]	0.65 [1]	0.61 [1]	0.62 [1]	0.65 [1]	0.62 [1]	0.64 [1]	0.64 [3]	0.67 [1]	0.63 [1]	0.62 [1]	0.60 [1]
O1	x	0.1143 [2]	0.1146 [1]	0.1144 [1]	0.1140 [1]	0.1145 [1]	0.1145 [1]	0.1147 [1]	0.1146 [1]	0.1145 [1]	0.1139 [1]	0.1149 [1]	0.1154 [1]	0.1160 [1]
	y	0.0870 [2]	0.0869 [1]	0.0867 [1]	0.0868 [1]	0.0870 [1]	0.0870 [1]	0.0870 [1]	0.0864 [1]	0.0863 [1]	0.0865 [1]	0.0872 [1]	0.0872 [1]	0.0873 [1]
	z	0.1394 [3]	0.1404 [2]	0.1397 [2]	0.1393 [2]	0.1394 [3]	0.1396 [2]	0.1403 [2]	0.1399 [2]	0.1398 [2]	0.1382 [3]	0.1408 [2]	0.1413 [3]	0.1429 [1]
	Beq	0.77 [4]	0.80 [2]	0.83 [2]	0.80 [2]	0.77 [3]	0.84 [2]	0.79 [2]	0.83 [3]	0.84 [3]	0.84 [3]	0.80 [2]	0.77 [3]	0.77 [2]
O2	x	0.3621 [2]	0.3617 [1]	0.3628 [1]	0.3627 [1]	0.3629 [1]	0.3632 [1]	0.3630 [1]	0.3628 [1]	0.3629 [1]	0.3632 [2]	0.3625 [1]	0.3626 [1]	0.3622 [1]
	y	0.2522 [2]	0.2520 [1]	0.2528 [1]	0.2530 [1]	0.2526 [2]	0.2522 [1]	0.2522 [1]	0.2523 [1]	0.2526 [1]	0.2534 [2]	0.2516 [1]	0.2510 [1]	0.2502 [1]
	z	0.3189 [4]	0.3186 [2]	0.3213 [2]	0.3213 [2]	0.3216 [3]	0.3226 [3]	0.3222 [2]	0.3213 [3]	0.3210 [3]	0.3217 [3]	0.3213 [2]	0.3217 [3]	0.3210 [2]
	Beq	0.96 [4]	0.98 [4]	1.09 [2]	1.06 [2]	1.04 [3]	1.12 [3]	1.09 [2]	1.12 [3]	1.14 [3]	1.22 [3]	1.06 [2]	1.03 [3]	1.01 [3]
O3	x	0.3512 [2]	0.3513 [1]	0.3516 [1]	0.3519 [1]	0.3517 [1]	0.3517 [1]	0.3516 [1]	0.3517 [1]	0.3518 [1]	0.3519 [1]	0.3515 [1]	0.3513 [1]	0.3510 [1]
	y	0.0183 [2]	0.0178 [1]	0.0186 [1]	0.0189 [1]	0.0189 [1]	0.0192 [1]	0.0188 [1]	0.0183 [1]	0.0184 [1]	0.0187 [2]	0.0186 [1]	0.0186 [1]	0.0184 [1]
	z	−0.0060 [4]	−0.0058 [2]	−0.0051 [2]	−0.0057 [2]	−0.0051 [3]	−0.0048 [2]	−0.0049 [2]	−0.0037 [2]	−0.0035 [2]	−0.0048 [2]	−0.0050 [2]	−0.0039 [3]	−0.0039 [2]
	Beq	0.77 [4]	0.89 [2]	0.92 [2]	0.92 [2]	0.94 [3]	0.97 [3]	0.92 [2]	0.93 [3]	0.93 [3]	1.02 [3]	0.94 [2]	0.89 [3]	0.87 [2]
*M*2′	Fe occ			0.006 [6]	0.010 [7]	0.006 [7]	0.008 [6]	0.008 [6]	0.010 [6]	0.045 [4]	0.008 [7]	0.006 [6]	0.006 [7]	0.009 [9]
	y			0.2216	0.2413	0.2220	0.2217	0.2219	0.2629	0.2216	0.2223	0.2217	0.2218	0.2417
	Beq			0.50	0.77	0.50	0.65	0.59	0.24	0.63	0.61	0.46	0.47	0.70

TABLE 4. Bond lengths and site volumes data for cpx of Ab-T and B-Ph suites. Atom position nomenclature after Burnham *et al.* (1967). Standard deviations in brackets. Other abbreviations as in Table 2

AB-T suite	VG3015					VG3106		VG3150			VG3151				VG3187	
	1	2	3	4	5	6	7	8	9	10	11	12	13	14	15	16
	Mc	Mr	Pc	Pr	gm	Mc	Pc	Mr	Pr	gm	Mc	Mr	Pc	Pr	Pc	Pr
*M*1–O1A1 (Å)	2.124 [1]	2.120 [1]	2.121 [1]	2.119 [1]	2.120 [1]	2.124 [1]	2.129 [1]	2.123 [1]	2.123 [1]	2.124 [1]	2.129 [1]	2.127 [1]	2.124 [1]	2.128 [1]	2.137 [2]	2.140 [1]
*M*1–O1A2 (Å)	2.049 [1]	2.051 [2]	2.051 [1]	2.045 [1]	2.048 [1]	2.048 [1]	2.055 [1]	2.053 [1]	2.050 [1]	2.052 [1]	2.057 [1]	2.058 [1]	2.054 [1]	2.057 [2]	2.075 [2]	2.077 [1]
*M*1–O2 (Å)	2.023 [1]	2.029 [1]	2.025 [1]	2.017 [1]	2.022 [1]	2.020 [1]	2.026 [1]	2.041 [1]	2.021 [1]	2.022 [1]	2.031 [1]	2.030 [1]	2.023 [1]	2.029 [1]	2.057 [1]	2.055 [1]
<*M*1–O> (Å)	2.066 [4]	2.066 [4]	2.066 [3]	2.060 [4]	2.063 [3]	2.064 [3]	2.070 [3]	2.072 [4]	2.065 [4]	2.066 [4]	2.072 [3]	2.072 [4]	2.067 [4]	2.072 [4]	2.090 [4]	2.091 [3]
V_{M1} (Å^3)	11.65 [1]	11.66 [1]	11.65 [1]	11.55 [1]	11.61 [1]	11.62 [1]	11.72 [1]	11.77 [1]	11.63	11.65 [1]	11.77 [1]	11.75 [1]	11.68 [1]	11.75 [1]	12.08 [1]	12.10 [1]
*M*2–O1 (Å)	2.349 [1]	2.347 [1]	2.352 [1]	2.345 [1]	2.351 [1]	2.348 [1]	2.347 [1]	2.344 [1]	2.351 [1]	2.350 [1]	2.343 [1]	2.347 [1]	2.348 [1]	2.347 [1]	2.348 [2]	2.349 [1]
*M*2–O2 (Å)	2.323 [1]	2.319 [1]	2.327 [1]	2.317 [2]	2.323 [1]	2.320 [1]	2.317 [1]	2.313 [1]	2.326 [1]	2.324 [1]	2.315 [1]	2.320 [1]	2.319 [1]	2.322 [2]	2.321 [2]	2.323 [1]
*M*2–O3C1 (Å)	2.566 [1]	2.571 [1]	2.566 [1]	2.563 [2]	2.565 [1]	2.566 [1]	2.574 [1]	2.578 [1]	2.565 [1]	2.569 [1]	2.577 [1]	2.576 [1]	2.571 [1]	2.578 [2]	2.591 [2]	2.591 [1]
*M*2–O3C2 (Å)	2.724 [1]	2.725 [1]	2.720 [1]	2.721 [1]	2.715 [1]	2.722 [1]	2.732 [1]	2.730 [1]	2.718 [1]	2.721 [1]	2.731 [1]	2.729 [1]	2.722 [1]	2.728 [1]	2.739 [1]	2.743 [1]
<*M*2–O> (Å)	2.490 [4]	2.490 [4]	2.491 [4]	2.487 [5]	2.489 [3]	2.489 [4]	2.492 [3]	2.491 [4]	2.490 [4]	2.490 [4]	2.492 [4]	2.493 [4]	2.490 [4]	2.494 [4]	2.500 [5]	2.501 [3]
<*M*2–O1,O2> (Å)*	2.336 [2]	2.333 [2]	2.339 [2]	2.331 [2]	2.337 [2]	2.334 [2]	2.332 [2]	2.328 [2]	2.338 [2]	2.337 [2]	2.329 [2]	2.333 [2]	2.333 [2]	2.334 [2]	2.334 [4]	2.336 [2]
<*M*2–O3> (Å)**	2.645 [2]	2.648 [2]	2.643 [2]	2.642 [2]	2.640 [2]	2.644 [2]	2.653 [2]	2.654 [2]	2.641 [2]	2.645 [2]	2.654 [2]	2.652 [2]	2.646 [2]	2.653 [2]	2.665 [3]	2.667 [2]
V_{M2} (Å^3)	25.50 [1]	25.48 [1]	25.53 [1]	25.38 [1]	25.45 [1]	25.45 [1]	25.54 [1]	25.51 [1]	25.48 [1]	25.52 [1]	25.51 [1]	25.56 [1]	25.48 [1]	25.59 [1]	25.75 [1]	25.81 [1]
T–±O1 (Å)	1.622 [1]	1.622 [1]	1.624 [1]	1.625 [1]	1.623 [1]	1.625 [1]	1.621 [1]	1.614 [1]	1.625 [1]	1.625 [1]	1.618 [1]	1.621 [1]	1.620 [1]	1.623 [1]	1.605 [1]	1.606 [1]
T–O2 (Å)	1.603 [1]	1.598 [1]	1.602 [1]	1.601 [2]	1.603 [1]	1.604 [1]	1.604 [1]	1.592 [1]	1.605 [1]	1.605 [1]	1.601 [1]	1.602 [1]	1.603 [1]	1.603 [2]	1.589 [2]	1.592 [1]
T–O3A1 (Å)	1.667 [1]	1.669 [1]	1.669 [1]	1.667 [1]	1.669 [1]	1.667 [1]	1.668 [1]	1.665 [1]	1.671 [1]	1.668 [1]	1.666 [1]	1.669 [1]	1.667 [1]	1.668 [1]	1.668 [1]	1.667 [1]
T–O3A2 (Å)	1.688 [1]	1.686 [2]	1.689 [1]	1.685 [2]	1.687 [1]	1.685 [1]	1.686 [1]	1.682 [1]	1.683 [1]	1.687 [1]	1.685 [1]	1.686 [1]	1.686 [1]	1.686 [2]	1.680 [2]	1.685 [1]
<*T*–O> (Å)	1.645 [3]	1.643 [3]	1.646 [2]	1.644 [3]	1.646 [2]	1.645 [3]	1.645 [2]	1.638 [3]	1.646 [3]	1.646 [2]	1.642 [2]	1.644 [3]	1.644 [3]	1.645 [3]	1.635 [3]	1.637 [2]
T–O_{nobrg} (Å)	1.612 [1]	1.610 [1]	1.613 [1]	1.613 [1]	1.613 [1]	1.615 [1]	1.612 [1]	1.603 [1]	1.615 [1]	1.615 [1]	1.609 [1]	1.612 [1]	1.612 [1]	1.613 [1]	1.597 [1]	1.599 [1]
T–O_{brg} (Å)	1.677 [2]	1.677 [2]	1.679 [2]	1.676 [2]	1.678 [2]	1.676 [2]	1.677 [2]	1.673 [2]	1.677 [2]	1.678 [2]	1.676 [2]	1.677 [2]	1.677 [2]	1.677 [2]	1.674 [2]	1.676 [2]
V_T (Å^3)	2.266 [2]	2.260 [2]	2.269 [2]	2.263 [2]	2.269 [2]	2.268 [2]	2.265 [2]	2.239 [2]	2.270 [2]	2.271 [2]	2.256 [2]	2.264 [2]	2.262 [2]	2.267 [2]	2.227 [2]	2.235 [2]

* <M2–O1,O2> = (M2–O1 + M2–O2)/2

** <M2–O3> = (M2–O3C1 + M2–O3C2)/2

TABLE 4 (*contd*)

B-Ph suite	VG3243		VG3022			VG3314		VG3276				VG3185	
	17	18	19	20	21	22	23	24	25	26	27	28	29
	Pc	Pc	Pc	Pr	gm	Pc	gm	Pc	Pr	gm	Mr	Pc	Pr
*M*1–O1A1 (Å)	2.125 [2]	2.124 [1]	2.124 [1]	2.124 [1]	2.126 [1]	2.126 [1]	2.126 [1]	2.121 [1]	2.120 [1]	2.122 [1]	2.128 [1]	2.131 [1]	2.133 [1]
*M*1–O1A2 (Å)	2.058 [2]	2.061 [1]	2.053 [1]	2.053 [1]	2.052 [1]	2.051 [1]	2.055 [1]	2.049 [1]	2.049 [1]	2.044 [1]	2.059 [1]	2.061 [1]	2.070 [1]
*M*1–O2 (Å)	2.026 [2]	2.031 [1]	2.019 [1]	2.018 [1]	2.021 [1]	2.022 [1]	2.024 [1]	2.020 [1]	2.016 [1]	2.009 [1]	2.032 [1]	2.037 [1]	2.046 [1]
<*M*1–O> (Å)	2.070 [5]	2.072 [3]	2.065 [3]	2.065 [3]	2.067 [3]	2.066 [3]	2.068 [3]	2.063 [3]	2.062 [3]	2.058 [4]	2.073 [3]	2.076 [3]	2.083 [3]
V_{M1} (Å^3)	11.71 [1]	11.75 [1]	11.63 [1]	11.63 [1]	11.66 [1]	11.66 [1]	11.70 [1]	11.60 [1]	11.58 [1]	11.51 [1]	11.78 [1]	11.84 [1]	11.96 [1]
*M*2–O1 (Å)	2.373 [2]	2.373 [1]	2.359 [1]	2.365 [1]	2.361 [1]	2.352 [1]	2.353 [1]	2.352 [1]	2.353 [1]	2.358 [1]	2.360 [1]	2.356 [1]	2.360 [1]
*M*2–O2 (Å)	2.361 [2]	2.361 [1]	2.339 [1]	2.345 [1]	2.338 [1]	2.327 [1]	2.330 [1]	2.329 [1]	2.331 [1]	2.334 [1]	2.338 [1]	2.331 [1]	2.335 [1]
*M*2–O3C1 (Å)	2.558 [2]	2.556 [1]	2.562 [1]	2.559 [1]	2.563 [1]	2.571 [1]	2.569 [1]	2.561 [1]	2.559 [1]	2.556 [1]	2.568 [1]	2.573 [1]	2.575 [1]
*M*2–O3C2 (Å)	2.709 [2]	2.714 [1]	2.717 [1]	2.707 [1]	2.714 [1]	2.719 [1]	2.721 [1]	2.727 [1]	2.726 [1]	2.714 [1]	2.719 [1]	2.730 [1]	2.732 [1]
<*M*2–O> (Å)	2.500 [5]	2.501 [3]	2.494 [3]	2.494 [3]	2.494 [4]	2.492 [3]	2.493 [3]	2.492 [3]	2.492 [3]	2.490 [4]	2.496 [3]	2.498 [4]	2.501 [3]
<*M*2–O1,O2> (Å)*	2.367 [4]	2.367 [2]	2.349 [2]	2.355 [2]	2.349 [2]	2.339 [2]	2.341 [2]	2.340 [2]	2.342 [2]	2.346 [2]	2.349 [2]	2.343 [2]	2.347 [2]
<*M*2–O3> (Å)**	2.633 [3]	2.635 [2]	2.639 [2]	2.633 [2]	2.638 [2]	2.645 [2]	2.645 [2]	2.644 [2]	2.642 [2]	2.635 [2]	2.643 [2]	2.651 [2]	2.653 [2]
V_{M2} (Å^3)	25.87 [1]	25.87 [1]	25.64 [1]	25.66 [1]	25.64 [1]	25.56 [1]	25.59 [1]	25.55 [1]	25.55 [1]	25.52 [1]	25.70 [1]	25.72 [1]	25.82 [1]
T–O1 (Å)	1.625 [2]	1.620 [1]	1.625 [1]	1.630 [1]	1.625 [1]	1.626 [1]	1.624 [1]	1.622 [1]	1.623 [1]	1.630 [1]	1.620 [1]	1.616 [1]	1.610 [1]
T–O2 (Å)	1.605 [1]	1.603 [1]	1.608 [1]	1.611 [1]	1.608 [1]	1.607 [1]	1.606 [1]	1.602 [1]	1.604 [1]	1.610 [1]	1.602 [1]	1.598 [1]	1.595 [1]
T–O3A1 (Å)	1.670 [2]	1.675 [1]	1.671 [1]	1.673 [1]	1.671 [1]	1.669 [1]	1.671 [1]	1.667 [1]	1.667 [1]	1.670 [1]	1.672 [1]	1.669 [1]	1.669 [1]
T–O3A2 (Å)	1.697 [2]	1.691 [1]	1.688 [1]	1.691 [1]	1.690 [1]	1.688 [1]	1.686 [1]	1.683 [1]	1.686 [1]	1.688 [1]	1.689 [1]	1.689 [1]	1.688 [1]
<*T*–O> (Å)	1.649 [3]	1.647 [2]	1.648 [2]	1.651 [2]	1.649 [2]	1.647 [2]	1.647 [2]	1.644 [2]	1.645 [3]	1.650 [3]	1.646 [2]	1.643 [2]	1.640 [2]
T–O_{nobrg} (Å)	1.615 [2]	1.611 [1]	1.617 [1]	1.621 [1]	1.617 [1]	1.616 [1]	1.615 [1]	1.612 [1]	1.614 [1]	1.620 [1]	1.611 [1]	1.607 [1]	1.602 [1]
T–O_{brg} (Å)	1.684 [2]	1.683 [2]	1.679 [2]	1.682 [2]	1.681 [2]	1.679 [2]	1.678 [2]	1.675 [2]	1.676 [2]	1.679 [2]	1.680 [2]	1.679 [2]	1.678 [2]
V_T (Å^3)	2.283 [2]	2.275 [2]	2.279 [2]	2.293 [2]	2.282 [2]	2.277 [2]	2.273 [2]	2.262 [2]	2.266 [2]	2.285 [2]	2.269 [2]	2.258 [2]	2.247 [2]

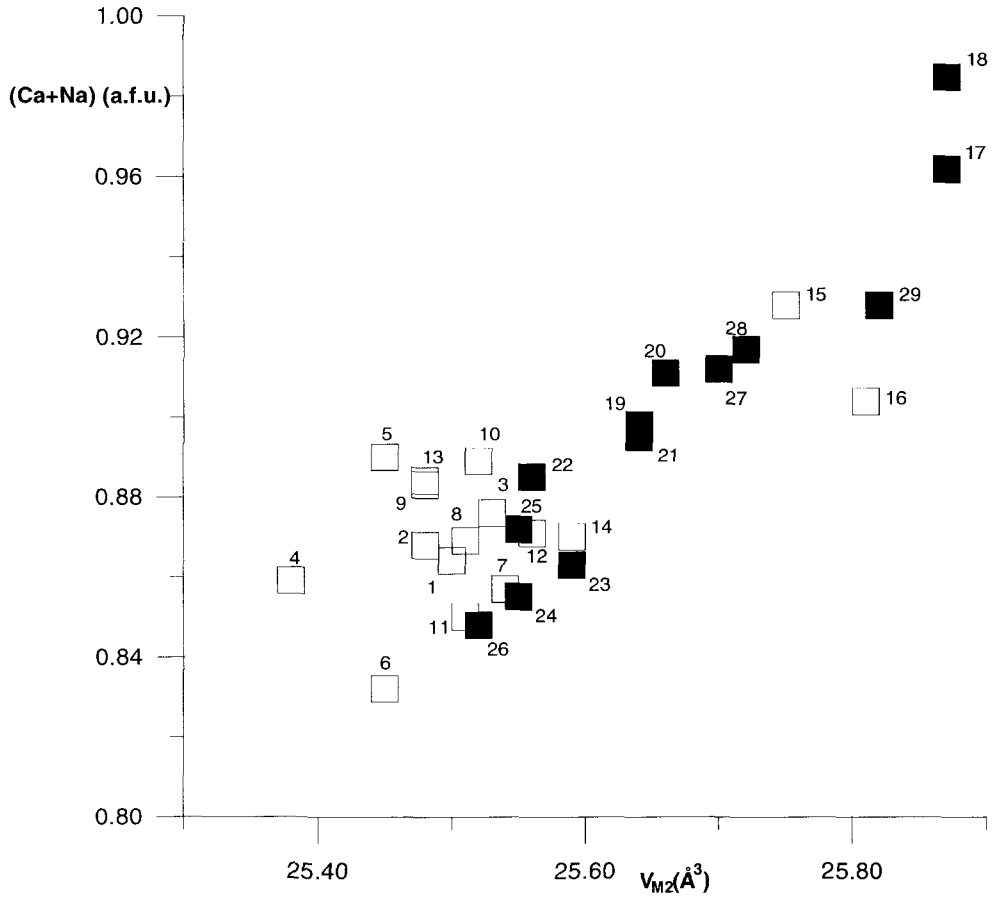

FIG. 4. Relationship between $M2$ site volume (V_{M2}) and (Ca+Na). Symbols as in Fig. 2.

crystals of the B-Ph suite with (Ca+Na) less than 0.90 a.f.u. for similar (Ca+Na) content, tend to have slightly higher V_{M2} than that of AB-T cpx (Fig. 4). The AB-T cpx are clearly distinct from the B-Ph cpx due to their shorter <$M2$–O1,O2> (less than 2.340 Å; Fig. 5*a*); there is a tendency for AB-T cpx to have longer <$M2$–O3> bond lengths (Fig. 6*a*), (Ca+Na) contents being the same.

For example, the shorter <$M2$–O3> (mean) bond length in crystal 26 relative to crystal 11 (Fig. 6*a*) is due to the former's higher Al^{IV} content in the T site, i.e. 0.235 *vs.* 0.151 a.f.u., respectively. The higher Al^{IV} in the T site of crystal 26 requires higher contents of R^{3+} in the $M1$ site, which induces greater shortening of the mean <$M1$–O> distance (crystal 26 = 2.058 Å; crystal 11 = 2.072 Å). The consequence is the greater length of the <$M2$–O1,O2> (mean) bond length in crystal 26 (2.346 Å) relative to crystal 11 (2.329 Å; Fig. 5*a*).

Discussion

Several works on pyroxene crystal chemistry have highlighted the fact that the polyhedral configurations of the $M1$, $M2$ and T sites are mutually dependent. The configurations of $M2$ and T polyhedra are constrained by (Ca+Na) and Al^{IV} contents, respectively. (Ca+Na) increase is generally accompanied by Al^{IV} increase. The charge balance is ensured by the increase of R^{3+} in the $M1$ site, when

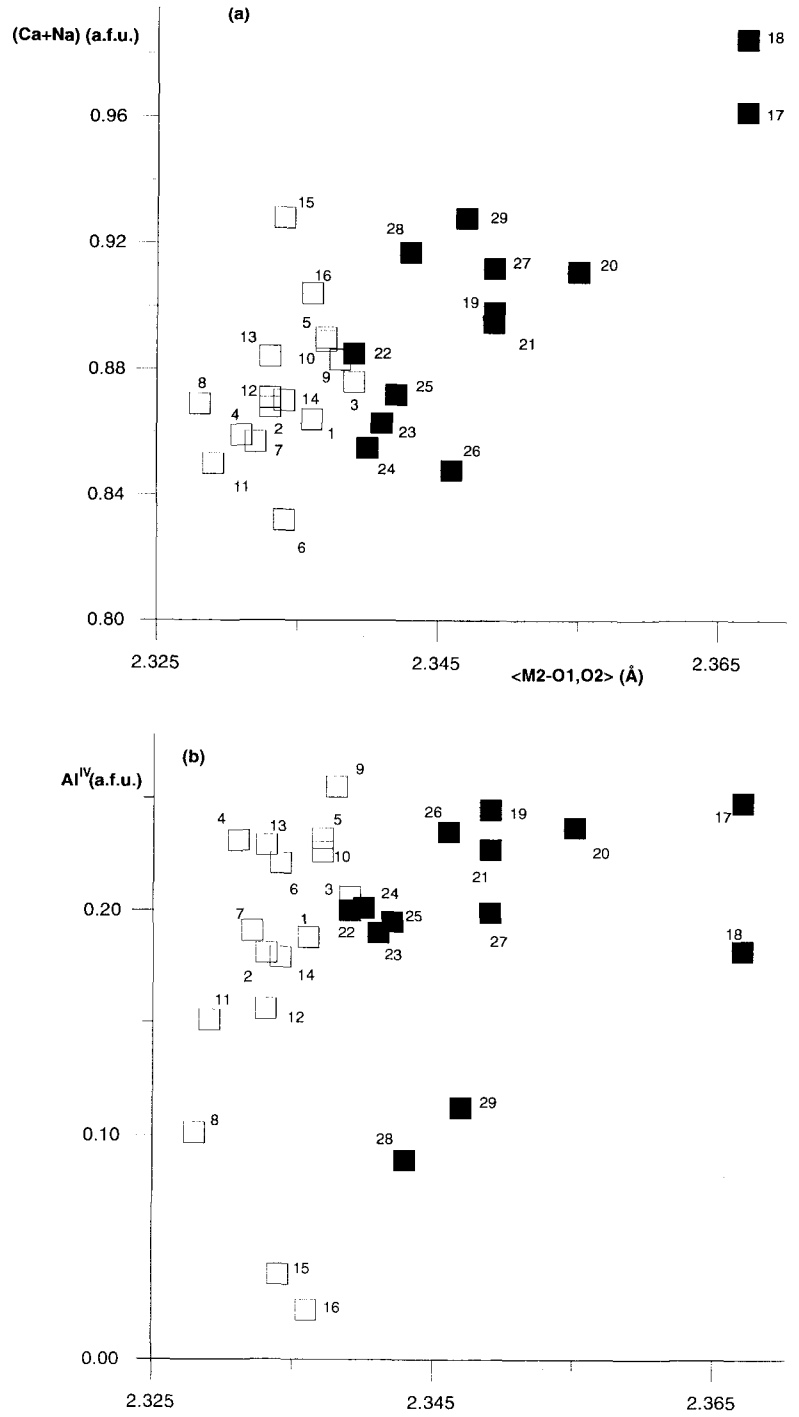

FIG. 5. Variations in <*M*2–O1,O2> bond lengths *vs.* (Ca+Na) (*a*) and Al^{IV} (*b*). Symbols as in Fig. 2.

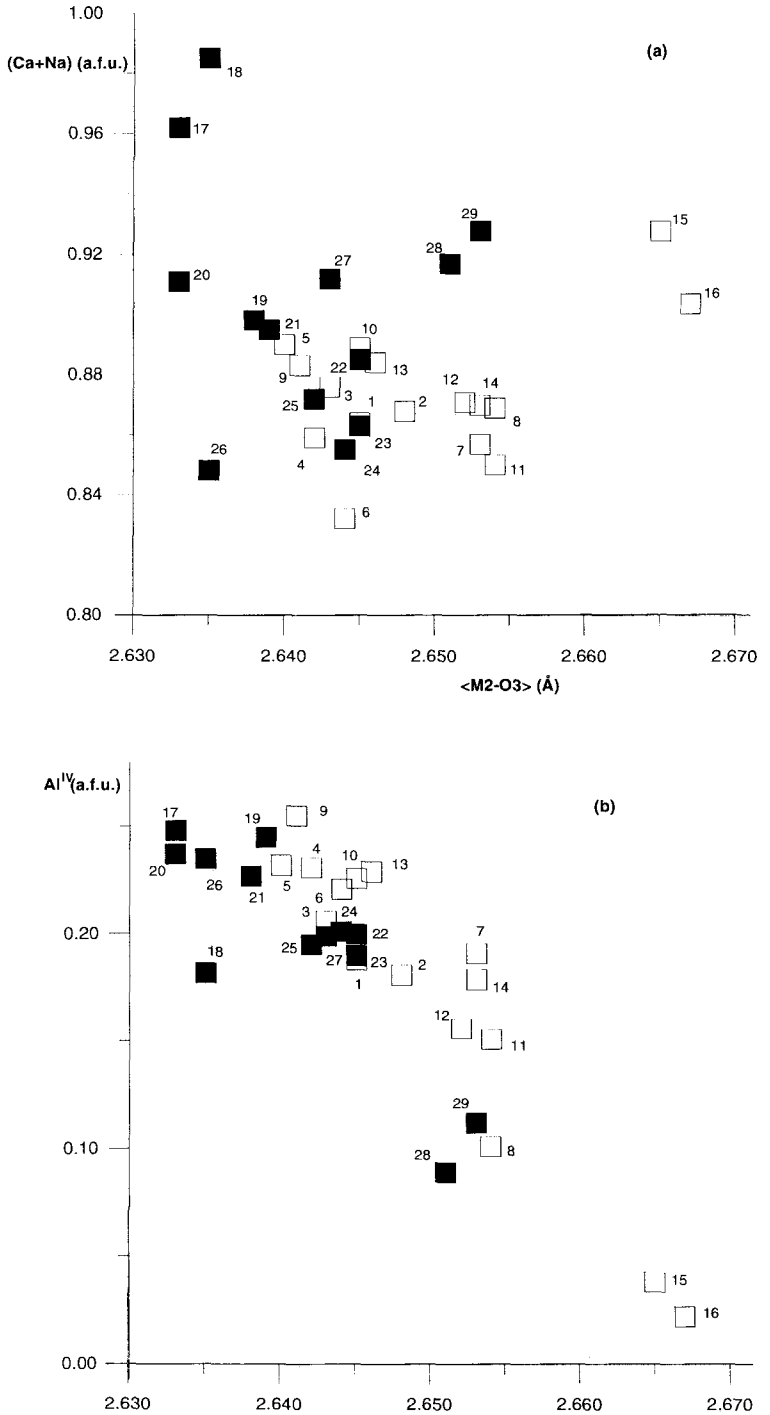

FIG. 6. Variations in <*M*2–O3> bond lengths *vs.* (Ca+Na) (*a*) and Al^{IV} (*b*). Symbols as in Fig. 2.

Na content is low. This cation distribution produces the lengthening of *M*2–O1, *M*2–O2, *T*–O1 and *T*–O2 bond lengths and the shortening of *M*2–O3 and *M*1–O bond lengths (Dal Negro *et al.*, 1989).

(Ca+Na) and Al^{IV} variations in the investigated cpx are not accompanied, however, by regular variations in *M*2–O bond lengths. For the crystals with (Ca+Na) content lower than 0.90 a.f.u., the bond lengths of the *M*2 polyhedron are poorly correlated with Al^{IV} content (Figs. 5*b* and 6*b*). There are several crystals with different Al^{IV} and (Ca+Na) contents but virtually identical <*M*2–O1,O2> bond lengths (e.g. crystals 6, 14 and 15 in the AB-T suite; 25 and 28, and 26 and 29 in the B-Ph suite). All these crystals show an increase in the (Ca+Na)/Al^{IV} ratio (3.8 to 24.4: AB-T suite; 4.5 to 10.3 and 3.6 to 8.3: B-Ph suite), due to both Al^{IV} decrease and (Ca+Na) increase. The decrease in Al^{IV} (*T*) is associated with R^{3+} (*M*1) decrease. For the above-mentioned crystals, the substitution of R^{3+} by Mg^{2+} and Fe^{2+} lengthens the *M*1–O bond lengths. Therefore, for each crystal group above mentioned, <*M*2–O1,O2> cannot lengthen, even though (Ca+Na) content increases (Fig. 5*a*). In addition, increasing Si^{4+} (*T*), the local charge balance around O3 oxygens is reached by means of the increase of <*M*2–O3> bond lengths, even though (Ca+Na) content increases (Fig. 6*a*).

In contrast to the above, there are crystals belonging to both B-Ph (28, 29, 18, 17) and AB-T (15, 16) suites which are characterized by high and quite constant (Ca+Na) (over 0.90 a.f.u.). These crystals show a good relationship between Al^{IV} and <*M*2–O1,O2> and <*M*2–O3> bond lengths (Figs. 5*b* and 6*b*). In addition, with increasing <*M*2–O1,O2> and decreasing <*M*2–O3>, (Ca+Na)/Al^{IV} ratio (41.1 to 3.9) decreases due to the increase of Al^{IV} (*T*) (0.022 to 0.248 a.f.u.). The Al^{IV} increase is balanced by the entry of R^{3+} (*M*1) which shortens *M*1–O bond lengths, so <*M*2–O1,O2> lengthens, even though (Ca+Na) contents remain virtually unchanged. In these crystals, the net charge of *T* site cations on O3 oxygens decreases and, even though the (Ca+Na) content is similar, this requires shortening of <*M*2–O3> bond lengths. Note that for different Al^{IV} the *T*–O3 bond lengths are virtually unchanged (Tables 2 and 4).

In summary, Al^{IV} (*T*) increase is correlated with *M*2–O bond lengths only if (Ca+Na) is almost constant (e.g. crystals 15 and 16 in the AB-T suite; 28 and 29 in the B-Ph suite) or the *M*2 site is nearly filled by (Ca+Na) (more than 0.96 a.f.u., e.g. crystals 17 and 18 in the B-Ph suite). On the contrary, when Al^{IV} (*T*) increases and (Ca+Na) decreases *M*2–O bond lengths are poorly correlated with Al^{IV} (*T*) content (e.g. crystals 15, 14, 6 in the AB-T suite or 28, 25 or 29, 26 in the B-Ph suite).

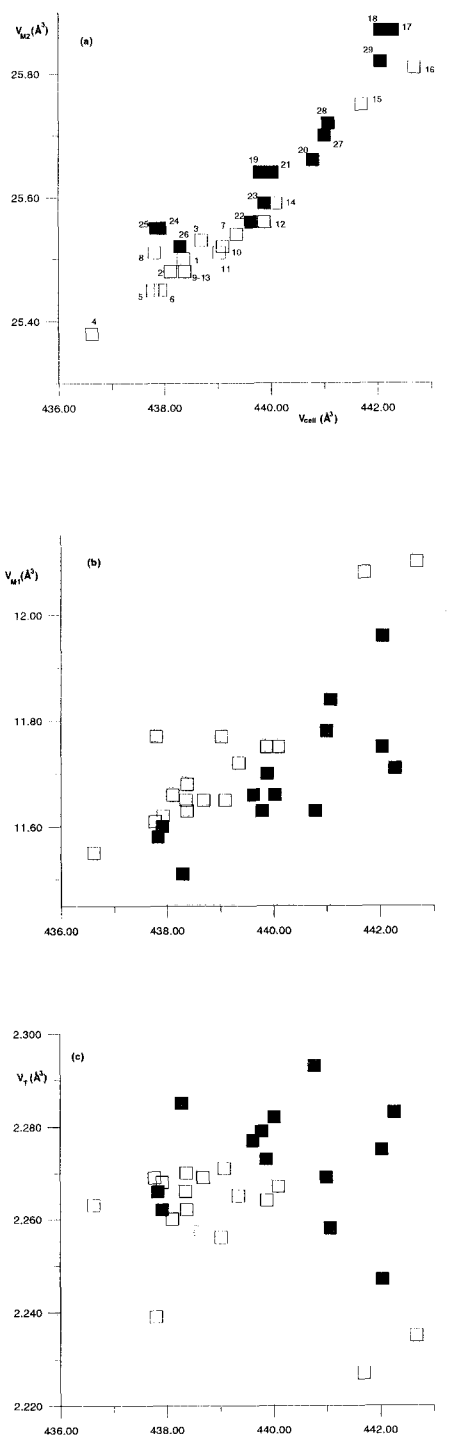

FIG. 7. Variations in cell volume (V_{cell}) *vs.* *M*2 (*a*), *M*1 (*b*) and *T* (*c*) site volumes. Symbols as in Fig. 2.

Concluding remarks

Variation of the *M*1 bond lengths depend only on R^{3+} content, necessary to balance the Al^{IV} in the *T* site. *M*1 geometric variations are similar in both B-Ph and AB-T cpx. On the other hand, the increase of Al^{IV} in the *T* site affects *M*2–O bond lengths in different ways, depending on (Ca+Na) content in the *M*2 site. Thus, the crystals with their *M*2 sites nearly filled by (Ca+Na) (more than 0.90 a.f.u.) show that *M*2–O bond length variations respond essentially to an increase of Al^{IV} in the *T* site (cf. Dal Negro *et al.*, 1985; Salviulo and Molin, 1993). Instead, the cpx with (Ca+Na) less than 0.90 a.f.u. show that Al^{IV} and (Ca+Na) increases are accompanied by a shortening of the <*M*2–O3> distance, while <*M*2–O1,O2> remains virtually unchanged.

It is noteworthy that variations in cell volume (V_{cell}) *vs.* site volumes (Fig. 7) clearly separate the cpx of the two suites and highlights the fact that the geometric features of cpx reflect the different alkaline character of the magmas.

The V_{cell} variations in the studied cpx are closely correlated with those of V_{M2} (i.e. (Ca+Na) content) (Fig. 7*a*) and to a lesser extent with those of V_{M1} (Fig. 7*b*). The V_{cell} variations do not appear to be correlated with those of V_T (Fig. 7*c*).

Except for one crystal, V_{cell} is higher than 437 Å^3, suggesting low pressure conditions (less than 10 kbar). An estimate of crystallization pressure for near-liquidus *C*2/*c* pyroxenes has been proposed by Nimis (1995) on the basis of the V_{cell}-V_{M1} relationship. In our cpx, we considered only the cores of the phenocrysts, which may be considered of near-liquidus crystallization. Fig. 8 shows that the maximum pressure of cpx crystallization for the basic rocks of B-Ph and AB-T suites is about 5 kbar. This low pressure is consistent with the petrography and evolved character (cf. Table 1) of these rocks. Note that the smallest V_{cell} (436.6 Å^3; Fig. 7), corresponding to *ca.* 8 kbar, is that of a late-crystallized cpx (crystal 4: rim), while the core (crystal 3) of the same phenocryst indicates a distinctly lower pressure (conservatively, *ca.*

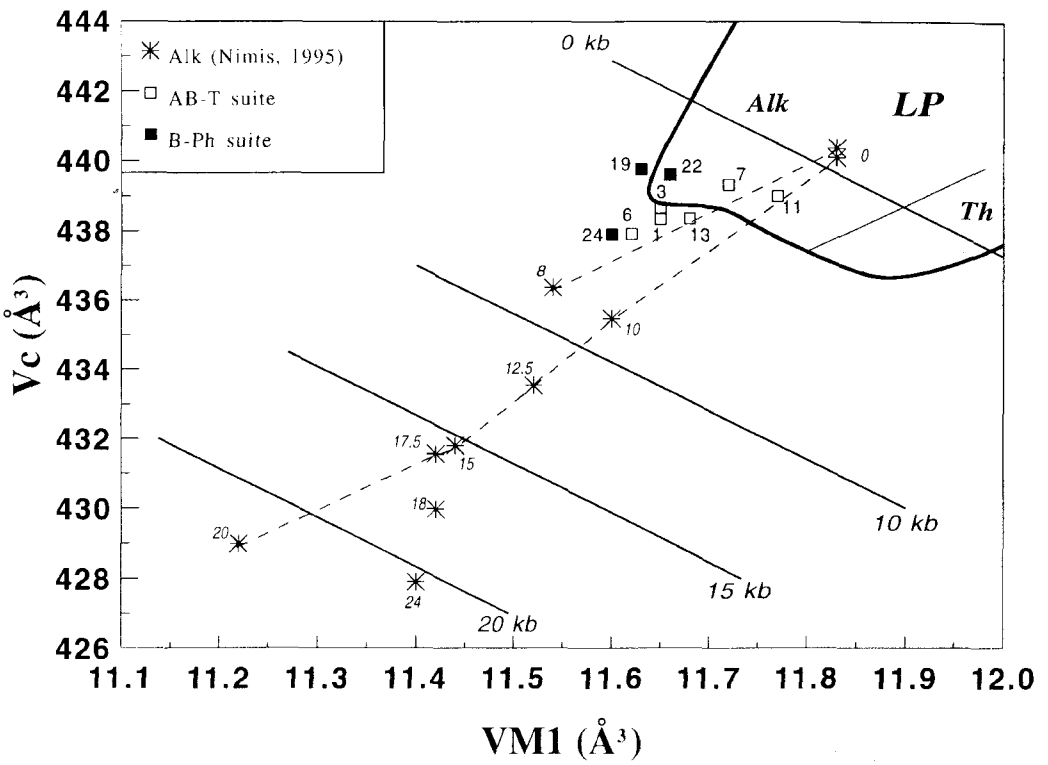

FIG. 8. Relationship between V_{M1} and cell volume (V_c) of phenocryst cores of the investigated cpx from basic rocks and those for alkaline *C*2/*c* pyroxenes (Nimis, 1995). LP = low pressure; Alk = alkaline; Th = tholeiitic fields (Dal Negro *et al.*, 1989); AB-T alkali-basalt- trachyphonolite suite (open squares); B-Ph = basanite-phonolite suite (filled squares).

2 kbar). Therefore, the differences in the crystal chemistry of cpx of early and late crystallization are not related to distinct pressure, but may reflect variation in melt composition and, possibly, the influence of other crystallizing mineral phases. Lastly, it must be stressed that even the largest cpx macrocrysts (*c.* 3–6 mm) crystallized in low-pressure conditions (less than 5 kbar).

Acknowledgements

The authors are grateful to Prof. G. Orsi (University of Naples) who kindly supplied the rock specimens (Italian Anctartica 3rd Expedition), and to Prof. L. Civetta (University of Naples), who provided the chemical analyses of the bulk rocks. We are much indebted to Prof. A. Dal Negro (University of Padova) who revised the manuscript and made useful comments and suggestions. The authors also acknowledge Dr. Prof. R.L. Oliver and an anonymous referee for their useful comments. Financial support came from the Ministero dell'Università e della Ricerca Scientifica e Tecnologica and the C.N.R. (Centro di Studio per la Geodinamica Alpina, Padova). This work has been carried out with the support of the Italian Programma Nazionale di Ricerche in Antartide.

References

Antonini, P., Civetta, L., Orsi, G., Piccirillo, E.M. and Bellieni, G. (1994) The Mount Melbourne and Mount Overlord subprovinces of the McMurdo Volcanic group (Northern Victoria Land — Antarctica): new geochemical and Sr-isotope data. *Terra Antarctica*, **1**, 115–9.

Burnham, C.W., Clark, J.R., Papike, J.J. and Prewitt, C.T. (1967) A proposed crystallographic nomenclature for clinopyroxene structures. *Z. Kristallogr.*, **125**, 109–19.

Dal Negro, A., Carbonin, S., Molin, G.M., Cundari, A. and Piccirillo, E.M. (1982) Intracrystalline cation distribution in natural clinopyroxenes of tholeiitic, transitional and alkaline basaltic rocks. In *Advances in Physical Geochemistry*, Vol. 2 (S.K. Saxena., ed.), Springer, Berlin Heidelberg New York, pp. 117–50.

Dal Negro, A., Carbonin, S., Salviulo, G., Piccirillo, E.M. and Cundari, A. (1985) Crystal chemistry and site configuration of clinopyroxene from leucite-bearing rocks and related genetic significance: the Sabatini lavas, Roman Region, Italy. *J. Petrol.*, **26**, 1027–40.

Dal Negro, A., Molin, G.M., Salviulo, G., Secco, L., Cundari, A. and Piccirillo, E.M. (1989) Crystal chemistry of clinopyroxene and its petrogenetic significance: a new approach. In *The Lithosphere in Italy. Advances in Earth Sciences Research.* Atti Convegni Lincei, Vol. 80 (A. Boriani, M. Bonafede, G.B. Piccardo and G.B. Vai, eds.), pp. 271–95.

De La Roche, H., Leterrier, P., Grandclaude, P. and Marchal, M. (1980) A classification of volcanic and plutonic rocks using R1–R2 diagram and major element analysis. Its relationships with current nomenclature. *Chem. Geol.*, **29**, 183–210.

Kyle, P.R. (1990) McMurdo Volcanic Group, Western Ross Embayment. In *Volcanoes of the Antarctic Plate of the Southern Oceans*. Am. Geoph. Un., Ant. Res. Ser. (W.E. Le Masurier and J.W. Thomson, eds.), Vol. 48, pp. 1–17.

Nimis, P. (1995) A clinopyroxene geobarometer for basaltic systems based on crystal-structure modeling. *Contrib. Mineral. Petrol.*, **121**, 115–25.

Papike, J.J., Cameron, K. and Baldwin, K. (1974) Amphiboles and pyroxenes: characterization of other than quadrilateral components and estimates of ferric iron from microprobe data. *Geol. Soc. Amer. Abstr. Prog.*, **6**, 1053–4.

Philips (1994) X40 Software for XRF analysis. Software Operation Manual, 7.34–7.38.

Salviulo, G. and Molin, G.M. (1993) Crystal-chemistry of clinopyroxene from Sunda Volcanic Arc. *Mineral. Petrol.*, **49**, 233–48.

Secco, L. (1988) Crystal-chemistry of high pressure clinopyroxene from spinel lherzolite nodules: Mts. Leura and Noorat suites, Victoria, Australia. *Mineral. Petrol.*, **39**, 175–85.

Shannon, R. D. (1976) Revised effective ionic radii and systematic studies of interatomic distances in halides and chalcogenides. *Acta Cryst.*, **A32**, 751–67.

[*Manuscript received 1 July 1996; revised 4 November 1996*]